Study on the eddy current damping of the spin dynamics of spatial debris from the Ariane launcher

Nicolas Praly, Nicolas Petit, Christophe Bonnal, Julien Laurent-Varin

Study on the eddy current damping of the spin dynamics of spatial debris from the Ariane launcher

Nicolas Praly⋆, Nicolas Petit⋆⋆, Christophe Bonnal⋆⋆⋆ and Julien Laurent-Varin⋆⋆⋆
⋆SYSNAV
57 Rue de Montigny, 27200 Vernon, France
⋆⋆ENSMP
CAS, 60-62 Boulevard Saint Michel, 75272 Paris cedex 06, France
⋆⋆⋆CNES
DLA, Rond Point de l'Espace, 91000 Evry, France

Abstract

This paper addresses the topic of damping of the spinning dynamics of a spatial debris orbiting around the Earth. Such debris, which can consists of parts of heavy launchers such as the Ariane rocket under consideration in this article, are impacted by torques generated by eddy currents as the conducting non-ferromagnetic body orbits through the Earth magnetosphere. Several previous works have focused on describing this induction phenomenon and have proposed analysis of empirical observations of this particular and important phenomenon which has attracted much attention since the number of spatial debris has emerged as a problem for the future of space programs, especially in low orbits. In this paper, we expose a relatively comprehensive modeling of the induction phenomenon, by means of Maxwell equations inside the conducting and non-ferromagnetic body. Through the generalized Ohm's law, we show how one can obtain a Neumann partial differential equations problem that, once solved, e.g. through a considered finite elements method, yields the value of induced currents and braking torques. The case of a spatial debris, being a part of a heavy launcher, having a cylindrical shape and thin walls is particularly studied. We show a methodology to estimate the decay-rate of the spinning velocity, which is proven to satisfy a first-order asymptotically stable linear dynamics. Special cases consisting of orbits of interest are treated.

1. Introduction

As the number of debris orbiting around the Earth has steadily increased since the early days of space programs, it seems that that a critical point has been reached in 2007 after the orbital explosion of the Chinese satellite ASAT which was followed in 2009 by the collision of the Iridium 33 satellite and Cosmos 2251 stage. These incidents are reported to have generated more than 4000 debris, of various sizes and shapes. In turn, future collisions of all the debris are expected to generate an increasing number of debris and significantly rise the chances of occurrence of damaging impacts on satellites and other spacecrafts, especially in low orbits. This problem has spurred a recent and strong interest for developing debris deorbiting technologies, in hope of alleviating the risk by removing, at least, the largest or the most dangerous debris. Various candidate solutions have been proposed. The vast majority of them presuppose the capture of the debris by the chaser prior to the deorbitation. In particular, nets [2], tether [5], solar sailing [7], booster [10] have been considered. Most of these envisioned technologies have in common poor robustness to the spinning dynamics of the debris under consideration. Indeed, it is quite difficult to attach a tether device to a spinning body, and it can reveal troublesome to catch a spinning debris with a net, especially in flat spin mode [13].

Interestingly, the effects of the Earth magnetic field can help here. At each instant, the permanent magnetic field from the magnetosphere generates eddy current in the spinning, conducting body. These induction-created currents generate, in turn, a torque opposed to the spinning of the body. Then, one can expect the initial rotation to damp over time, and eventually, asymptotically stabilize to zero. The purpose of this article is to expose a method to establish the damped dynamics of the debris in rotation along one of its axis an orbiting along the Earth. The geometry under consideration can be relatively general, but the case we put much of our attention on is a thin-wall cylindric body,

closed at the two ends by thin-wall half-spheres (we call this geometry "capsule"). This is representative of the debris stemming from the body of the heavy launcher Ariane.

We start from Maxwell equations and consider the generalized Ohm equation to relate the density of current to the exerted magnetic field. Using the obtained equation inside and on the boundary of the conducting body (which is assumed to be non-ferromagnetic and not the subject of self induction), we constitute a general Neumann partial differential equations problem in the electric potential variable. Once solved, e.g. thanks to a finite element method, this equation determines, through some straightforward differential calculus, the density of induced current from which the braking torque can be computed. In general, the spinning dynamics takes the form of a first-order asymptotically stable linear differential equation in the rotation velocity variable. The damping rate is numerically determined through the previously discussed method. The study is complemented by integrating this damped equation along orbits of reference, which defines the orientation and the strength of the exerted magnetic field. This serves to estimate the decay-rate of the initial spin, for various orbits and various size of debris.

The paper is organized as follows. In section 2, we give a brief overview of the literature on space debris, by exposing the risk of collision that they generate, the nature of the debris, their number and their density in various parts of the near-space domain. We also give an outlook on the currently envisioned de-orbiting or capture technologies. In section 3, we show how to determine the discussed Neumann problem for such a conducting debris. The example of capsule bodies is illustrated. We also explain how this problem can be treated numerically with a finite-element solver. Examples of the obtainable accuracy are given, for particular cases of conducting bodies where an analytic solution exists, e.g. a rotating sphere. In section 4, we establish the damped differential equation and solve it along orbits and for bodies of particular interest. Numerical results covering orbits typically used by the Ariane launcher debris are reported.

2. The problem of space debris

Since the beginning of the Space Conquest in 1957, human space activity produced a large amount of debris. The origins of those objects are quite various : sources range from satellites that are no longer working to objects produced by a launch mission (last stage of a launch vehicle, separation device to name a few). Actually, more than known 15500 debris are listed, most of them being in the same orbit as satellites in use. Unfortunately debris larger than 1 mm can cause critical damage to a satellite. Even if most of the recent satellites have avoidance capabilities, the procedure of avoidance cannot be initiated if the debris size is less than 0.1 m because the debris can not be detected.

Nearly 20 years ago the first article was published on the risk of cascading effect due to collisions between debris in Low Earth region. At that time, this phenomenon, named since the "Kessler Syndrome" [6], was not considered as a serious threat. Today, due to multiple collisions between orbital bodies, this effect is well known and all the space agencies over the world are working together to develop mitigation strategies. The current situation is, in some aspects, alarming because our ability to use outer space in long term is not guaranteed. New rules and regulations have been set to limit the lifetime of objects in outer space, but older debris which are on stable orbit will stay and eventually produce more debris through collisions. Simulation have proven that the situation cannot be improved unless some of the debris are actually removed neatly [9]. Reducing the number of objects is now a necessity to ensure the sustainability of our space activities. The most polluted area is the low Earth orbit. The removal must begin with massive objects which have the largest collision probabilities, typically vehicle stages or satellites that out-of-order. The geometry of those objects is well-known and offers a solid interface which is advantageous if catching is considered. On the other hand the attitude is not known and the current technologies do not allow to catch objects which rotate faster than a few degrees per seconde. Launcher upper stage are usually passivated at the end of their life in order to reduce the risk of explosion due to overpressure in fuel tanks, but this venting potentially imparts to the stage an angular movement which can reach a few tens of degrees per second; such high values would probably prevent the capture of the stage with current technologies. Several of the most promising solutions baseline the capture of the debris with a robotic arm before equipping it with a deorbitation kit such as an electrodynamic tether [5], an drag augmentation surface or a solar sail [7]. Other conceivable solutions use a spacetug to push or pull the debris in the Earth's atmosphere without using a robotic arm, but nevertheless with prior control of the debris dynamics. Finally, one can note that even contactless solutions such as the use of laser beam to "push" or "destroy" the object may be strongly perturbated by a high rotation speed of the debris. For the vast majority of the conceivable solutions, high angular velocities represent a limiting factor potentially killing the most promising concepts.

Since 1957 observations on the rotation period have been made for satellites and rocket bodies. Various studies [14], [1] show that the rotation period increases exponentially over time. The increase have various origins : friction

due to the remaining fuel in the tanks, eddy current torque, air drag (for trajectories having altitude below 500 km). This phenomenon is of great importance for any future "catching mission" because, even if the debris have a high rotation speed at the beginning of its life, the rotation will decrease over time. The only question that remains is to evaluate its decay time. The answer will be given in this paper for Ariane 4 H10 stages.

To determine the relaxation time we study the eddy current torque produced by a debris rotating in the Earth's magnetic field. Other eddy current torques have already been calculated : for a spherical body in the historical article of H. Hertz in 1880 "On induction in rotating spheres" [3], for a spherical body in the book "Static and dynamic electricity" in 1950 by W. R. Smythe [12] (the formula is different because it accounts for the self-induction in the sphere), for an hollow cylinder by G. L. Smith in a NASA report [11]. As we will see it, our modern numerical tools allow to calculate torques for any geometry using finite-elements methods.

3. Equations governing the magnetic induction phenomenon inside a spinning conduction non-ferromagnetic body

Induction can be described by Maxwell's equations, involving the potential associated to the electric and magnetic fields, the expression of the Lorentz force and Ohm's law. We define the following notations included in the table 1.

Table 1: Nomenclature

Symb.	Quantity	Unit	Symb.	Quantity	Unit
$\vec{E}(M,t)$	Electric field	$V.m^{-1}$	$V(M,t)$	Electric potential	V
$\vec{B}(M,t)$	Magnetic field	T or G	$\vec{A}(M,t)$	Magnetic vector potential	$T.m$
$\rho(M,t)$	Total charge density	$C.m^{-3}$	q	Charge of a particle	C
$\vec{j}(M,t)$	Total current density	$A.m^{-2}$	$\kappa(M,t)$	Resistivity of a material	$\Omega.m$
μ_0	Permeability of free space	$H.m^{-1}$	ε_0	Permittivity of free space	$C.V^{-1}.m^{-1}$
$\vec{F}(M,t)$	Lorentz force	N	$\vec{\Gamma}(M,t)$	Torque	$N.m$
$\vec{v}(M,t)$	Speed	$m.s^{-1}$	ω	Rotation speed	$^\circ.s^{-1}$ or $rad.s^{-1}$
Ω	Volume of a conducting material	m^3	$d\tau$	Mesoscopic volume	m^3
Ω_s	Surface of a conducting material	m^2	$\bar{\bar{I}}$	Inertia tensor	$kg.m^2$
$\vec{n}(M)$	Normal vector to Ω_s	-			

3.1 Basic equations

Before formulating the problem of induction, we introduce the basic equations we will use later : under the hypothesis of small variation in time, Maxwell's equations are $div_M(\vec{E}(M,t)) = \rho(M,t)/\varepsilon_0$, $div_M(\vec{B}(M,t)) = 0$, $\overrightarrow{rot}_M(\vec{B}(M,t)) = \mu_0\vec{j}(M,t)$ and $\overrightarrow{rot}_M(\vec{E}(M,t)) = -\partial\vec{B}(M,t)/\partial t$. The charge conservation $div_M(\vec{j}(M,t)) = 0$ is verified by the previous Maxwell's equations. The properties of the electromagnetic field enable us to introduce the electric potential and magnetic vector potential :

$$\vec{E}(M,t) = -\overrightarrow{grad}_M\left(V(M,t)\right) - \frac{\partial\vec{A}}{\partial t} \text{ and } \vec{B}(M,t) = \overrightarrow{rot}_M\vec{A}(M,t). \tag{1}$$

We can also introduce the Lorentz Force :

$$\vec{F} = q\left(\vec{E}(M,t) + \vec{v}\wedge\vec{B}(M,t)\right). \tag{2}$$

With equations (1) and (2), generalized local Ohm's law is

$$\kappa\vec{j}(M,t) = -\overrightarrow{grad}_M\left(V(M,t)\right) - \frac{\partial\vec{A}(M,t)}{\partial t} + \vec{v}(M,t)\wedge\vec{B}(M,t). \tag{3}$$

3.2 Typical induction problem

We consider a volume Ω, each point M of Ω moves at speed $\vec{v}(M,t)$ through a constant magnetic field. Moreover we consider that the self-induction phenomenon is negligible, the only magnetic field we consider is the stationary Earth's magnetic field. We also assume that the magnetic field is spatially homogeneous (constant) at the scale of an object, so $\vec{B}(M,t) = \vec{B}_0$. The current inside this volume verifies Ohm's law (3). As we consider a stationary magnetic field this equation becomes :

$$\kappa \vec{j}(M,t) = -\overrightarrow{grad}_M\left(V(M,t)\right) + \vec{v}(M,t) \wedge \vec{B}_0. \tag{4}$$

The current inside Ω verifies these two properties :

1. $div_M\left(\vec{j}(M,t)\right) = 0 \quad \forall M \in \Omega$ (charge conservation),

2. $\vec{j}(M,t).\vec{n}(M) = 0 \quad \forall M \in \Omega_s$ (the current stays inside the volume).

To determine the current inside Ω, one has to find the potential $V(M)$. The two previous properties applied to the simplified Ohm's law (4) give a typical Neumann's problem :

$$\begin{cases} \nabla^2 V(M) = F(M) & \forall M \in \Omega \\ \frac{\partial V(P)}{\partial n}\Big|_{\Omega_s} = f(P) & \forall P \in \Omega_s. \end{cases} \tag{5}$$

This problem can be solved through a Green's function. The Green's function must follow some properties one can find in the reference [8] and is unique. The potential which is solution to the problem (5) is :

$$V(M_0) = -\int_\Omega G(M,M_0) F d\Omega - \int_{\Omega_s} G(P,M_0) f(P) d\Omega_s + constant \tag{6}$$

It means that if one finds a solution to the problem (5) then this solution is unique. The constant does not really matter in our case because, classically, it is the gradient of the potential that creates the current.

Once the current is known, the torque created by the current inside Ω is found through the expression of the Lorentz force (2). The torque created at a point P by a mesoscopic volume with a density current $\vec{j}(M,t)$ through a magnetic field $\vec{B}(M,t)$ is :

$$\frac{d\vec{\Gamma}}{d\tau} = P\vec{M} \wedge \left(\vec{j}(M,t) \wedge \vec{B}(M,t)\right). \tag{7}$$

We can summarize the method to find the torque created by eddy current in a conducting material as followed :

1. Formulate simplified Ohm's law (4) for the conducting material,

2. Apply the two properties of the current inside a conducting material to the simplified Ohm's law to get a typical Neumann's problem on the electric potential,

3. Solve the Neumann's problem (5),

4. Reformulate the simplified Ohm's law with the expression of the electric potential to find the current density in the material,

5. Evaluate the torque (7).

One critical point in this method is to solve Neumann's-problem. In fact there are few cases where the solution can be analytically determined. A sphere is one of the few geometry where a simple analytical solution exists. Most of the time the solution is much more complicated. Finite-elements is a method that enables us to solve this kind of problem with any geometry. We use such method to evaluate the torque created by eddy current in a capsule in section 3.3. As there is an analytical solution for spherical bodies, the finite-elements solver performance can be evaluated for the induction problem. Typical errors evaluated between the solver and the analytical values are less than 2% of the torque created by eddy currents.

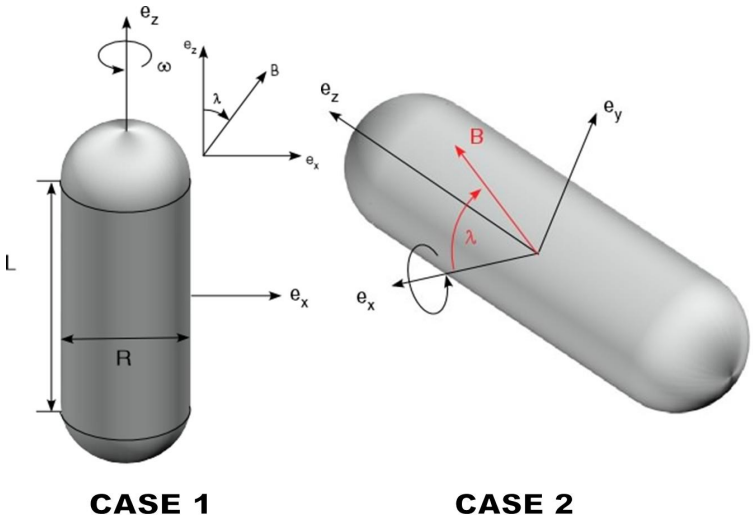

Figure 1: Definition of the notations for a capsule rotating along its longitudinal axis and along its transverse axis.

3.3 Induction problem applied to a capsule

The capsule is a thin-wall cylindric body closed at the two ends by thin-wall half-spheres. The length of the cylinder is L, its radius R and its thickness e. The two half spherical shells have the same radius and thickness as the cylindrical part. To determine the torque induced by eddy currents two cases must be considered : the first case we study is the capsule rotating along its longitudinal axis, the second is the same capsule rotating along a transverse axis.

Case 1 : capsule rotating along its longitudinal axis

We use the same system coordinates as the sphere. The Oz axis is the longitudinal axis of the capsule. The rotation speed along this axis is ω. The magnetic field is $\vec{B}(M,t) = B(\sin\lambda\vec{e}_x + \cos\lambda\vec{e}_z)$. We define (j_x, j_y, j_z) the components of $\vec{j}(M,t)$ in cartesian coordinates. Moreover we neglect the self-induction phenomenon.

We use the methodology described in the previous sections :

1. We apply the simplified Ohm's law (4) to the rotating sphere, we obtain

$$\begin{cases} \kappa j_x = -\frac{\partial V}{\partial x} + \omega x \cos\lambda B \\ \kappa j_y = -\frac{\partial V}{\partial y} + \omega y \cos\lambda B \\ \kappa j_z = -\frac{\partial V}{\partial z} - \omega x \sin\lambda B \end{cases} \tag{8}$$

2. If we apply the two properties of the current in the volume and at its surface, the Neumann's problem for a rotating capsule is

$$\begin{cases} \nabla^2 V = 2\omega B\cos\lambda \\ x\frac{\partial V}{\partial x} + y\frac{\partial V}{\partial y} = \omega(x^2+y^2)B\cos\lambda & \underbrace{r=R \text{ and } r=R-e}_{\text{cylindrical part}} \\ x\frac{\partial V}{\partial x} + y\frac{\partial V}{\partial y} + \left(z-\frac{L}{2}\right)\frac{\partial V}{\partial z} = \\ \qquad \omega(x^2+y^2)B\cos\lambda - \omega\left(z-\frac{L}{2}\right)xB\sin\lambda & \underbrace{r=R \text{ and } r=R-e}_{\text{high half-sphere}} \\ x\frac{\partial V}{\partial x} + y\frac{\partial V}{\partial y} + \left(z+\frac{L}{2}\right)\frac{\partial V}{\partial z} = \\ \qquad \omega(x^2+y^2)B\cos\lambda - \omega\left(z+\frac{L}{2}\right)xB\sin\lambda & \underbrace{r=R \text{ and } r=R-e}_{\text{low half-sphere}}. \end{cases} \tag{9}$$

3. We split the potential in two parts : a potential V_1 that depends of $\cos\lambda$ and a potential V_2 that depends of $\sin\lambda$. There is a trivial solution for V_1 but V_2 must be determined through the finite-elements method. The potential is

$$V = \omega\frac{(x^2+y^2)}{2}\cos\lambda B + V_2,$$

where V_2 is the solution of the reduced problem

$$\begin{cases} \nabla^2 V_2 = 0 \\ x\frac{\partial V_2}{\partial x} + y\frac{\partial V_2}{\partial y} = 0 & \underbrace{r = R \text{ and } r = R - e}_{\text{cylindrical part}} \\ x\frac{\partial V_2}{\partial x} + y\frac{\partial V_2}{\partial y} + \left(z - \frac{L}{2}\right)\frac{\partial V_2}{\partial z} = -\omega\left(z - \frac{L}{2}\right)xB\sin\lambda & \underbrace{r = R \text{ and } r = R - e}_{\text{high half-sphere}} \\ x\frac{\partial V_2}{\partial x} + y\frac{\partial V_2}{\partial y} + \left(z + \frac{L}{2}\right)\frac{\partial V_2}{\partial z} = -\omega\left(z + \frac{L}{2}\right)xB\sin\lambda & \underbrace{r = R \text{ and } r = R - e}_{\text{low half-sphere}}. \end{cases} \tag{10}$$

The finite-elements solver gives a value of the torque induced by eddy currents. By linearizing around a geometry we can find an "analytical" expression of the torque in the body coordinate system.

4. This step is directly done with the finite-elements solver.

5. The torque linearized in the body coordinate system is

$$\underbrace{\vec{\Gamma}_b \approx -\frac{\omega B^2}{\kappa}\sin^2\lambda\left(\pi e L R^3 + \frac{\pi}{3}eR^4\right)\vec{e}_k}_{R\sim 1.3\ m \quad L=5\leftrightarrow 7\ m \quad e\ll R}. \tag{11}$$

Case 2 : capsule rotating along its transverse axis

We use the same capsule. This time the rotation takes place about the Ox axis at the speed ω. Once more we neglect the self-induction. The following coordinates systems is used :

- (e_x, e_y, e_z) is a fixed coordinate system, the magnetic field in constant in this system and in the $x0y$ plane. The capsule is rotating along the e_x axis.
- (e_i, e_j, e_k) is a body coordinate system link to the capsule. e_x axis et e_i axis are merged. e_k axis is the longitudinal axis of the capsule.
- (e_r, e_θ, e_k) is used as a cylindrical coordinate system linked to the capsule.

The magnetic field is

$$\vec{B}(M,t) = B(\cos\lambda\vec{e}_x + \sin\lambda\vec{e}_y).$$

1. We apply the simplified Ohm's law (4) to the rotating sphere, we obtain

$$\begin{cases} \kappa j_i = -\frac{\partial V}{\partial x} + \omega z\sin\lambda\sin(\omega t)B - \omega y\sin\lambda\cos(\omega t)B \\ \kappa j_j = -\frac{\partial V}{\partial y} + \omega y\cos\lambda B \\ \kappa j_k = -\frac{\partial V}{\partial z} + \omega z\cos\lambda B \end{cases} \tag{12}$$

2. We apply the current properties to the simplified Ohm's law (12). We find the following Neumann's problem

$$\begin{cases} \nabla^2 V = 2\omega B\cos\lambda \\ x\frac{\partial V}{\partial x} + y\frac{\partial V}{\partial y} = \omega z x\sin\lambda\sin(\omega t)B \\ \qquad -\omega xy\sin\lambda\cos(\omega t)B + \omega y^2\cos\lambda B & \underbrace{r = R \text{ and } r = R - e}_{\text{cylindrical part}} \\ x\frac{\partial V}{\partial x} + y\frac{\partial V}{\partial y} + \left(z - \frac{L}{2}\right)\frac{\partial V}{\partial z} = \omega z x\sin\lambda\sin(\omega t)B \\ \qquad -\omega xy\sin\lambda\cos(\omega t)B + \omega y^2\cos\lambda B \\ \qquad +\omega z\left(z - \frac{L}{2}\right)\cos\lambda B & \underbrace{r = R \text{ and } r = R - e}_{\text{high half-sphere}} \\ x\frac{\partial V}{\partial x} + y\frac{\partial V}{\partial y} + \left(z + \frac{L}{2}\right)\frac{\partial V}{\partial z} = \omega z x\sin\lambda\sin(\omega t)B \\ \qquad -\omega xy\sin\lambda\cos(\omega t)B + \omega y^2\cos\lambda B \\ \qquad +\omega z\left(z + \frac{L}{2}\right)\cos\lambda B & \underbrace{r = R \text{ and } r = R - e}_{\text{low half-sphere}}. \end{cases} \tag{13}$$

3. We can split the potential in 3 parts : a potential V_1 that doesn't depend of time, a potential V_2 that depends of $\cos(\omega t)$ and a potential V_3 that depends of $\sin(\omega t)$. There are trivial solutions for V_1 and V_2, but V_3 must be find through the finite-elements method. The potential is

$$V(x,y,z) = \frac{B\omega\left(z^2+y^2\right)\cos\lambda}{2} - \frac{Bxy\omega\cos(\omega t)\sin\lambda}{2} + V_3,$$

where V_3 is the solution of the reduced Neumann's problem

$$\begin{cases} \nabla^2 V_3 = 0 \\ x\frac{\partial V_3}{\partial x} + y\frac{\partial V_3}{\partial y} = \omega z x \sin\lambda\sin(\omega t)B & \underbrace{r=R \text{ and } r=R-e}_{\text{cylindrical part}} \\ x\frac{\partial V_3}{\partial x} + y\frac{\partial V_3}{\partial y} + \left(z-\frac{L}{2}\right)\frac{\partial V_3}{\partial z} = \omega z x \sin\lambda\sin(\omega t)B & \underbrace{r=R \text{ and } r=R-e}_{\text{high half-sphere}} \\ x\frac{\partial V_3}{\partial x} + y\frac{\partial V_3}{\partial y} + \left(z+\frac{L}{2}\right)\frac{\partial V_3}{\partial z} = \omega z x \sin\lambda\sin(\omega t)B & \underbrace{r=R \text{ and } r=R-e}_{\text{low half-sphere}}. \end{cases} \tag{14}$$

As the previous case, we can find a linearized "analytical" torque formula through the finite-elements solver.

4. This step is directly done with the finite-elements solver.

5. The torque linearized in the body coordinate system is

$$\underbrace{\vec{\Gamma}_b \approx \frac{\omega B^2}{\kappa}\sin^2\lambda\left(\frac{3}{4}\pi e L R^3 + \frac{5}{6}\pi e R^4\right)\vec{e}_k}_{R\sim 1.3\ m \quad L=5\leftrightarrow 7\ m \quad e\ll R}. \tag{15}$$

4. Damping of spinning dynamics along orbits of interest

4.1 Description of interesting orbits and its environmental conditions

We now study debris from Ariane 4 stages. Those stages called H10 were initially on sun synchronous orbits with altitudes ranging from 500 to 800 km; therefore the orbit's inclinaison is approximately 97 to 98°. We use the IGRF 2005 (with the 2010 coefficients) magnetic model so as to simulate the internal Earth's magnetic field without modeling the time variation (time variation does not change the value of the magnetic more than 0.1% in a year). This model gives us the direction and the intensity of the magnetic field at each point of the orbit. Figure 2 shows a typical stage trajectory (the trajectory is in the Earth's rotating coordinate system) and the intensity of the magnetic field at the same altitude computed with the IGRF model.

The intensity of the magnetic field for a typical H10 orbit is between 0.1G at equator and 0.55G at poles. We neglect the air drag torque and suppose that passivation was correctly done so as to ignore fuel friction in tanks. We assume that the only torque except the eddy current torque is the gravity gradient torque.

4.2 Axial spin study

We simulate the attitude dynamic of a debris submitted to a gravity gradient and an eddy current torques. We assume that the longitudinal axis of the debris coincides with its linear speed vector. The debris is rotating along this axis at the speed ω_0. These two assumptions represent the initial attitude conditions of the debris. The attitude dynamic equation reads

$$\dot{\vec{\omega}} = \bar{\bar{I}}^{-1}\left(\vec{\Gamma} - \vec{\omega}\otimes\bar{\bar{I}}\vec{\omega}\right), \tag{16}$$

where $\vec{\Gamma} = \vec{\Gamma}_{gg} + \vec{\Gamma}_{ec}$. $\vec{\Gamma}_{gg}$ represents the gravity gradient torque and $\vec{\Gamma}_{ec}$ the eddy current torque. This torque is equal in the body coordinate system to

$$\vec{\Gamma}_{ec} = \begin{pmatrix} -\frac{1}{\kappa}\left(\pi e L R^3 + \frac{\pi}{3}eR^4\right)\omega_i\left(B_j^2+B_k^2\right) \\ -\frac{1}{\kappa}\left(\frac{3}{4}\pi e L R^3 + \frac{5}{6}\pi e R^4\right)\omega_j\left(B_i^2+B_k^2\right) \\ -\frac{1}{\kappa}\left(\frac{3}{4}\pi e L R^3 + \frac{5}{6}\pi e R^4\right)\omega_k\left(B_i^2+B_j^2\right) \end{pmatrix}_b, \tag{17}$$

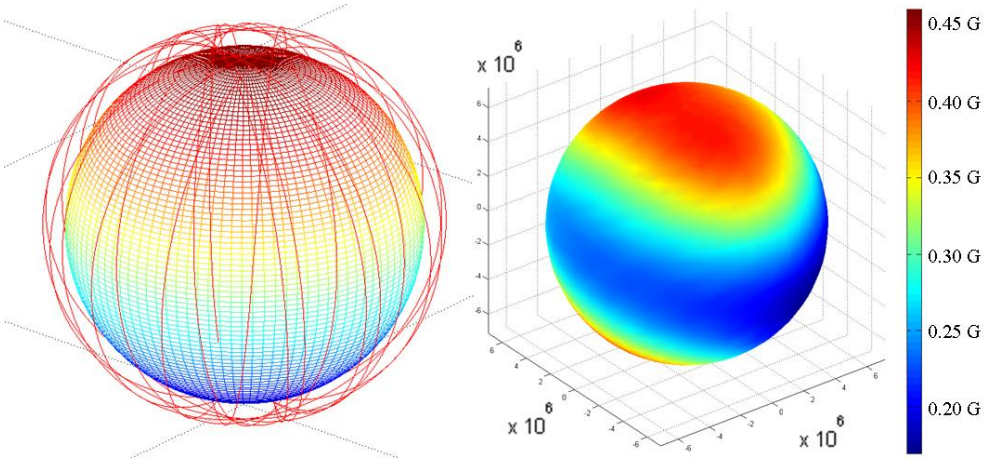

Figure 2: Stages trajectory and intensity of the magnetic field encountered

where (B_i, B_j, B_k) are the components of the Earth's magnetic field in the body coordinate system, $(\omega_i, \omega_j, \omega_k)$ the components of $\vec{\omega}$ in the same coordinate system.

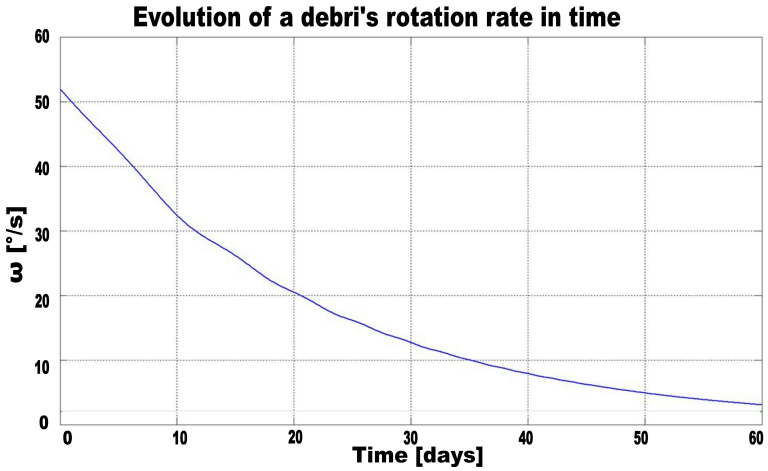

Figure 3: Attitude simulation for the flight 35 H10 stage.

Figure 3 reports the result of the simulation with the flight 35 orbits and $\omega_0 = 52°/s$ (this is approximately the speed rotation measured for this H10 stages). The inertia tensor used for this simulation is taken from Ariane 4 datasheet [4]. The rotation speed decreases exponentially as observed for other space bodies. This simulation illustrates the phenomenon of eddy current rotation damping. The following table 2 includes the result of other simulations. All simulations presents an identical exponentially-decreasing tendency. The evaluated time of decay concerning an H10 stage is between 20 and 25 days.

4.3 Flat spin study

The axial spin configuration is the initial rotation's configuration. Due to multiple factors, e.g. fuel friction in tanks, the initial axial spin configuration can rapidly change to a flat spin configuration. In order to evaluate the time of decay, we simulate the flat spin initial condition using the same torque equation (17). The rotation also decreases exponentially but the time of decay is much longer than the axial spin configuration as pointed out in the table 3.

Table 2: Axial spin simulation results

Flight	**Apogee (km)**	**Perigee (km)**	**Initial Speed** ($^\circ/s$)	**Decay's time (day)**
V35	779	764	52	25
V44	764	760	60	25
V52	798	782	38	22
V72	774	766	39	25
V75	625	594	60	19
V107	789	783	37.5	22
V124	623	610	42	23

Table 3: Flat spin simulation results

Flight	**Initial Speed** ($^\circ/s$)	**Decay's time (day)**
V52	20	190
V107	20	225

4.4 Time of decay

Whatever the rotation's configuration, an eddy current torque is induced in a conducting body rotating in a homogeneous magnetic field. The resolution of the attitude dynamic equation for an aluminium H10 stages in LEO points out an exponential decrease on the angular rate. The time of decay is strongly related to the rotation's configuration but is lower than 250 days. Leaning on the simulations and the few observations, there is great hope to find conducting debris with a low angular rate after few years in near-Earth space.

5. Observation of debris movements

The following step in the study of the residual movement of old debris in orbit is naturally the observation, in order to validate the results presented above and verify that one can expect the targets for Active Debris Removal to be relatively steady, therefore easily catchable. Such observations can be done in situ, with orbital assets approaching the target to observe with optical or radar means its 3 rotational degrees of freedom, or can be led from ground, again with optical or radar means. As currently there is no available orbital system capable of monitoring the movement of satellites, or at least as such results are not publicly available, the only capability offered today is from ground.

5.1 Radar observation

Numerous radars can be considered for the observation of the debris. One of the most efficient is the TIRA from FGAN, in Germany; it is capable of providing kinematics of large objects with a precision in the range of $0.1^\circ/s$ in all directions, as was mentioned for instance by Kawamoto and al. [15]. This large radar will unfortunately not be available for such measures before some times.

A formal request for observation has been issued to the US JSpOC, but so far has not led to any results either.

Another request has been sent to the French Ministry of Defence to use the ship "Le Monge" to make several observations of a selected batch of old Ariane upper stages. The requirements were to have two observation periods per object lasting more than 5 minutes with a precision better than 1 second, with different sight angles in order to guarantee a good 3D vision. These series of observations have effectively been performed at the end of May 2011, considering two upper stages, corresponding to the Ariane flights V75 and V107; as shown in Table 2, these upper stages had initial rotation velocities of respectively $60^\circ/s$ and $37.5^\circ/s$.

5.2 Amateur observations

Several networks of amateur astronomes do publish their observations on the web. A typical example, very rich, is given in [16]. The provided information gives details on the observation conditions and dates, azimuths, magnitude

and magnitude fluctuation. They also provide a qualitative information relative to the movement of the object. As an example, the Ariane upper stage of flight V75 has been reported 4 times, with magnitudes between 4 and 5, and a movement quoted as "Steady" or "Almost Steady". This information is particularly interesting. Table 4 gives a synthesis of the movements of all the Ariane upper stages left in Low Earth Orbit, according to [16]. It describes from left to right the COSPAR catalog number of the object, the name of the debris and its launch date, the orbital parameters (Apogee, Perigee, Inclination), its international number, the number of reported observations, the magnitude variability and the magnitude, the date of the last observation, and the general comment on the movement of the debris. One can see from this table that the vast majority of the debris are noted as Steady or Almost Steady. Unfortunately, these observations are not really quantified, and giving qualitative results. Furthermore, most of the observations are relatively old now, most of them being done shortly after the launch, and it would be very interesting to refresh them. Nevertheless, it seems obvious that they testify of a clear damping of the rotational movement of the debris, and tend to validate the "magnetic damping" assumption.

Table 4: Synthesis of observations devoted to old Ariane upper stages [16]

Num.	Name	launch	Za (m)	Zp (m)	i (°)	Int. Nb.	Obs.	Movement	Magnitude	Last Obs.	Remarks
2004-049H	ARIANE 5 R/B V165	18/12/2004	705298	570330	98.31	28499	1	S	+2.5	23/06/2005	
2002-009B	ARIANE 5 R/B V145	01/03/2002	797761	749554	98.18	27387	7	S	+4 to +5.5	17/09/2005	1st obs period 39s, 4th obs almost S
1999-064C	ARIANE 40 R/B V124	03/12/1999	620639	609394	98.12	25979	1	S	4	16/01/2005	
1998-017B	ARIANE 40 R/B V107	24/03/1998	787823	782406	98.25	25261	14	S	+2 to +5	10/09/2000	
1995-033D	ARIANE 40+3 R/B V75	07/07/1995	622743	592284	98.28	23608	4	S or almost S	+4 to +5	17/04/1999	2 obs. almost S
1995-021B	ARIANE 40+ R/B V72	21/04/1995	775265	764971	98.52	23561	52	Variable to S	+2.5 to 7	07/12/2001	initial periods 45 to 90 s then S
1993-061H	ARIANE 40 R/B V59	26/09/1993	798394	781406	98.66	22830	10	S	+3 to 5	11/02/1999	4th obs. S or long period
1992-052D	ARIANE 42P R/B V52	10/08/1992	1408489	1292382	66.06	22079	5	Undetermined	+3.5 to 8	02/05/1994	2 obs. variable, period 60s
1991-050F	ARIANE 40 R/B V44	17/07/1991	762516	759238	98.72	21610	61	S at the end	+3.5 to 8	04/09/2005	rapidly variying 12s then almost S
1990-005H	ARIANE 40 R/B V35	22/01/1990	777352	763655	98.67	20443	24	S at the end	+4.3 to 6	06/09/1997	rapidly variying 20s then S
1986-019C	ARIANE 1 R/B V16	22/02/1986	797522	781000	98.89	16615	6	S at the end	+3 to 7	28/08/2007	tumbling (breakup) then S

5.3 IADC action

Considering the relatively low reliability of the information published so far, the international community has decided to start an action at IADC level; the IADC (International Agencies Space Debris Coordination Committee [17]) is a technical Working Group joining the 12 major Space Agencies, meeting once a year. Its Working Group 1 is devoted to measurements, radar and optical, aiming mainly at giving data to the other Working Groups. During its 29th meeting held in Berlin (Germany) in April 2011, the action to systematically observe the movement of large debris has been undertaken. It should lead, by 2012, to professional, updated and repeated observations, enabling the validation of the theoretical studies and a comprehensive list of stable large debris, aim of the future Active Debris Removal actions.

6. Conclusion

The number of spatial debris has emerged as a problem for the future of space programs. Numerous solutions to limit the number of debris in low Earth orbit are under study but one of the major problems in the development concerns the angular rate of the debris. In this paper, we exposed a general modeling of the induction phenomenon leading to the spinning's damping of a spatial conducting debris in the Earth magnetic field. The general method is then applied to an aluminium H10 stage geometry. The evaluated eddy-current braking torque is used in an attitude simulator on a low Earth orbit to evaluate the decay time of a typical H10 stage which is found lower than 250 days.

The previous papers on the subject, the few observations and the results of this article shows a natural angular rate's damping of a conducting debris in low Earth orbit. The time of decay is strongly related to the debris geometry, material and rotation configuration but it is strongly conceivable to find debris with a low angular rate after few years in space.

Acknowledgements

This study was performed under R&T CNES contract.

The authors wish to thank CNES for financial support, and David Vissière and Mathieu Hillion from SYSNAV for their technical support.

References

[1] Boehnhardt, H., Koehnhke, H. and Seidel, A. 1989, The acceleration and the deceleration of the tumbling period of Rocket Intercosmos 11 during the first two years after launch, *Astrophysics and Space Science*, vol. 162, no. 2, p. 297-313.

[2] 2011, Description of the ROGER project, *www.esa.int*

[3] Hertz, H. 1896, On induction In rotating spheres, *Miscellaneous Papers*.

[4] 1994, Dossier de définition Troisième étage H10 III, *A4-DF-1300000-D*.

[5] Ishige, Y., Kawamoto, S. and Kibe, S. 2004, Study on electrodynamic tether system for space debris removal, *Acta Astronautica*, V. 55, Issue 11, p. 917-929

[6] Kessler, D. J. and Burton, G. 1978, Collision Frequency of Artificial Satellites: The Creation of a Debris Belt, *Journal of Geophysical Research*.

[7] Lappas, V. , Adeli, N. , Fernandez, J. , Theodorou, T. , Visagie., L., Steyn, H., Le Couls, O. , and Perren., M. 2010, Cubesail: A low cost small cubesat mission for de-orbiting leo objects, *Small Satellites Systems and Services*

[8] Lebedev, N., and Al. 1979, Worked problems in applied mathematics, *Dover Publications*.

[9] Liou, J.-C., Johnson, N.L. and Hill, N.M. 2010, Controlling the growth of future LEO debris populations with active debris removal, *Acta Astronautica*, V. 66, Issues 5-6, p. 648-653

[10] Ruault, JM., Desjean, MC. ,Bonnal, C. and Bultel, P. 2010, Active Debris Removal (ADR): From identification of problematics to in flight demonstration preparation, *1st European Workshop On Active Debris Removal*

[11] Smith, G. L. 1962, A theoretical study of the torques induced by a magnetic field on rotating cylinders and spinning thin wall cones, cone frustrums, and general bodies of revolution, *NASA. TR-R-129*.

[12] Smythe, W. R. 1950, Static and dynamic electricity, *London: McGraw-Hill*, 2nd ed.

[13] Wertz, J. R. 1980, Spacecraft Attitude Determination and Control, *Astrophysics and Space Science Library*, p.501

[14] Wilson, R. H. Jr. 1977, Magnetic effects on space vehicles and other celestial bodies, *The Irish Astronomical Journal*, Vol 13, n° 1/2.

[15] Kawamoto, S., Ohkawa, Y., Nishida, S., Kitamura, S., Kibe, S., Hanada, T., Mine, M., 2009, *Strategies and Technologies for Cost Effective Removal of Large Sized Debris*, Proceedings of the International Conference on Orbital Debris Removal.

[16] 2011, Amateur observations, *http://www.io.com/ mmccants/ppas/index.html*

[17] 2011, Inter-Agency Space Debris Coordination Committee, *http://www.iadc-online.org*